Chapter 11

Ultrafast Measurement Techniques

11.1 Pump Probe Measurements

11.1.1 Non-Colinear Pump-Probe Measurement:

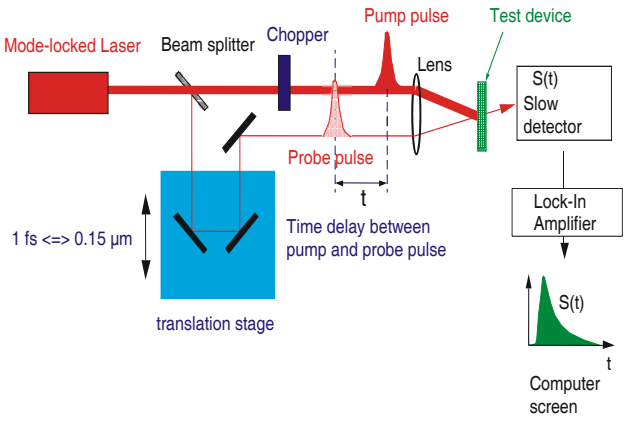

Figure 11.1: Non-colinear pump-probe setup with co-polarized pump-probe beams.
Adapted from U. Keller.

Figure 11.1 shows a non-colinear pump-probe measurement setup. To suppress background light and low frequency noise of the probe beam the pump

beam is chopped. Typical chopper frequencies of regular mechanical choppers are $f_{ch} = 100Hz - 2kHz$. Mechanical choppers up to 20kHz have been built. With acousto-optic modulators or electro-optic modulators chopper freuqencies up to several hundred MHz are possible.

Lets denote $S_{in} = S_0 + \delta S$ as the probe pulse energy, where S_0 is the average value and δs a low frequency noise of the pulse source and $S(t)$ is the probe signal transmitted through the test device. Then the detected signal transmitted through the test device can be written as

$$\begin{aligned} S(t) &= T(P(t))S_{in} \\ &= T_0 S_{in} + \frac{dT}{dP}\left(P_0 m(t)\right) \end{aligned} \tag{11.1}$$

where T_0 is the transmission without pump pulse, P_0 is the pump pulse energy and $m(t)$ the chopper modulation function. It is obvious that if the noise of the probe laser δS is of low freuqency, then the signal can be shifted away from this noise floor by chosing an appropriately large chopper frequency in $m(t)$. Ideally, the chopper frequency is chosen large enough to enable shot noise limited detection.

Sometimes the test devices or samples have a rough surface and pump light scattered from the surface might hit the detector. This can be partially suppressed by orthogonal pump and probe polarization

This is a standard technique to understand relaxation dynamics in condensed matter, such as carrier relaxation processes in semiconductors for example.

11.1.2 Colinear Pump-Probe Measurement:

Sometimes pump and probe pulses have to be collinear, for example when pump probe measurements of waveguide devices have to be performed. Then pump and probe pulse, which might both be at the same center wavelength have to be made separable. This can be achieved by using orthogonal pump and probe polarization as shown in Figure 11.2 or by chopping pump and probe at different frequencies and detecting at the difference frequency, see Figure 11.3.

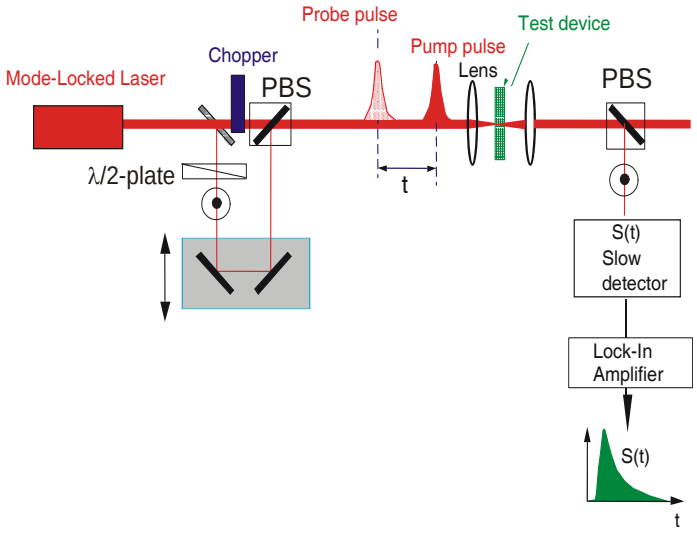

Figure 11.2: Colinear pump-probe with orthogonally polarized pump and probe beams.
Adapted from U. Keller.

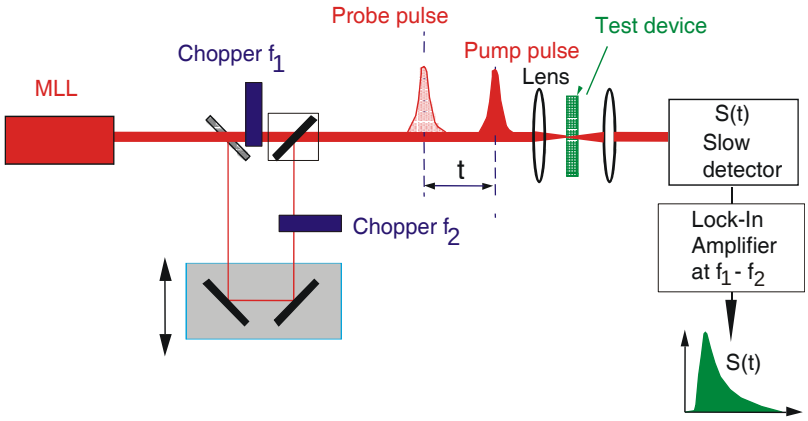

Figure 11.3: Colinear pump probe with chopping of pump and probe and lock-in detection at the difference frequency.
Adapted from U. Keller.

11.1.3 Heterodyne Pump Probe

The lock-in detection is greatly improved if the difference frequency at which the detection occurs can be chosen higher and the signal can be filtered much better using a heterodyne receiver. This is shown in Figure 11.4, where AOM's are used to prepare a probe and reference pulse shiftet by 39 and 40 MHz respectively. The pump beam is chopped at 1kHz. After the test device the probe and reference pulse are overlayed with each other by delaying the reference pulse in a Michelson-Interferometer. The beat note at 1MHz is downconverted to base band with a receiver.

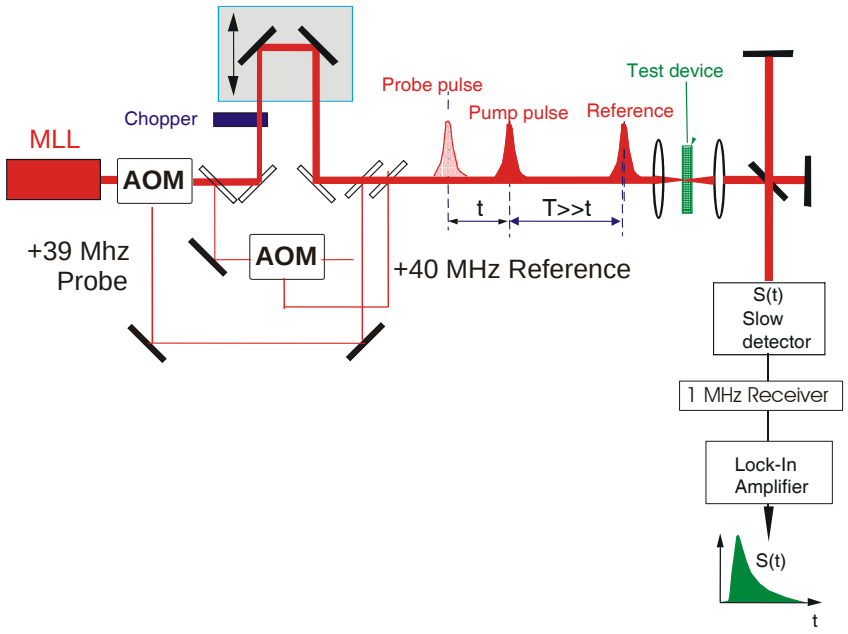

Figure 11.4: Colinear pump probe measurement with parallel polarization and large difference frequency.
Adapted from U. Keller.

If a AM or FM receiver is used and the interferometers generating the reference and probe pulse are interferometerically stable, both amplitude and phase nonlinearities can be detected with high signal to noise.

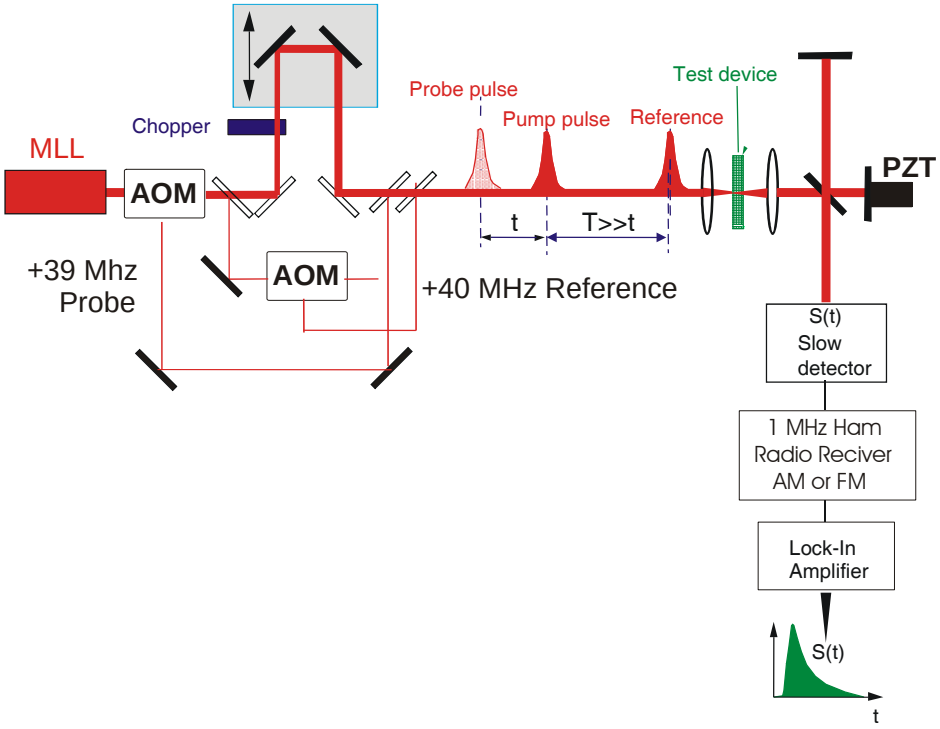

Figure 11.5: Heterodyne pump probe using AM and FM receiver to detect amplitude and phase nonlinearities.
Adapted from U. Keller.

11.2 Electro-Optic Sampling:

Electro-Optic Sampling was invented by Valdmanis and Mourou in the early 1980's [8][5]. Its is based on polarization rotation of a short laser pulse when propagating in a medium showing a linear electro-optic effect. The polarization rotation is due to an applied electric filed, i.e. the optical pulse samples the instantaneous electric field, see Fig.11.6

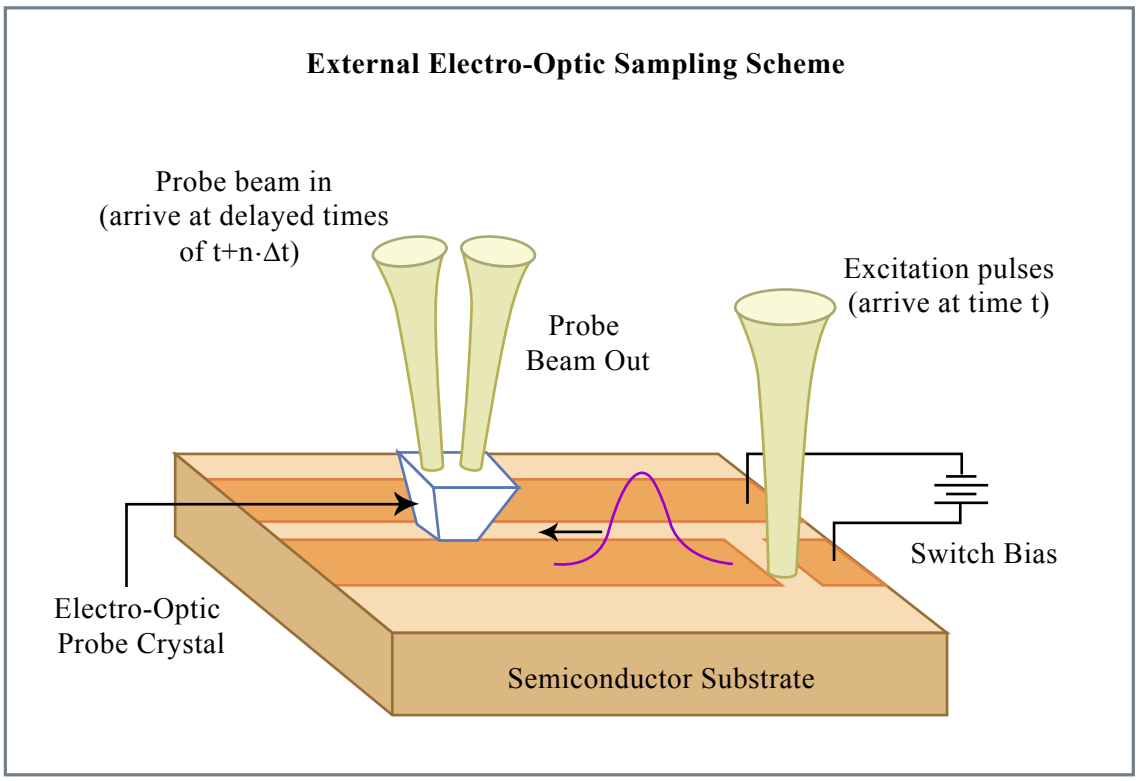

Figure 11.6: Electro-optic sampling scheme according ot J. Whitaker, Univ. of Michigan, Ann Arbor.

Figure by MIT OCW.

In Fig. 11.6 a electic transient is generated with a photo-conductive switch activated by a femtosecond laser pulse. A delayed pulse samples the transient electronic pulse with an electro-optic probe as shown in Fig. 11.7.

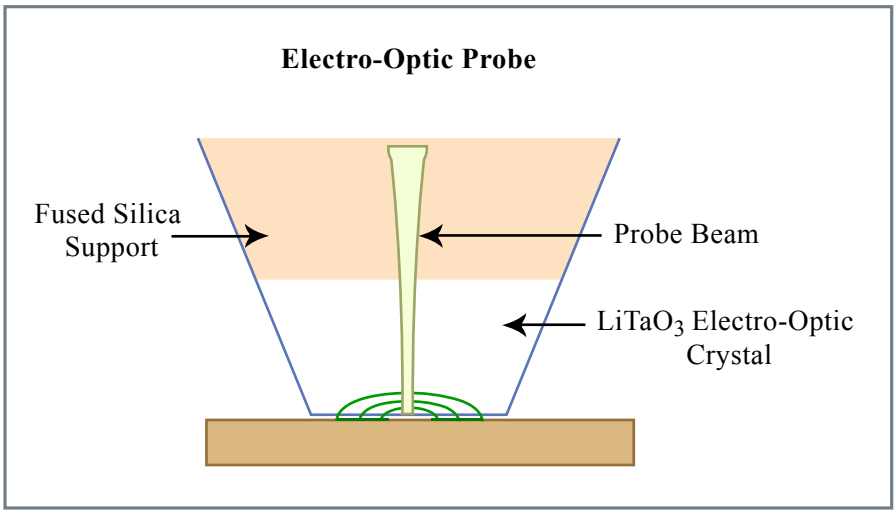

Figure 11.7: $LiTaO_3$−Electro-Otpic Probe according to J. Whitaker, Univ. Michigan.

Figure by MIT OCW.

Fig. 11.8 shows an overal version of an electro-optic sampling system according to J. Whitaker, Univ. of Michigan [6]

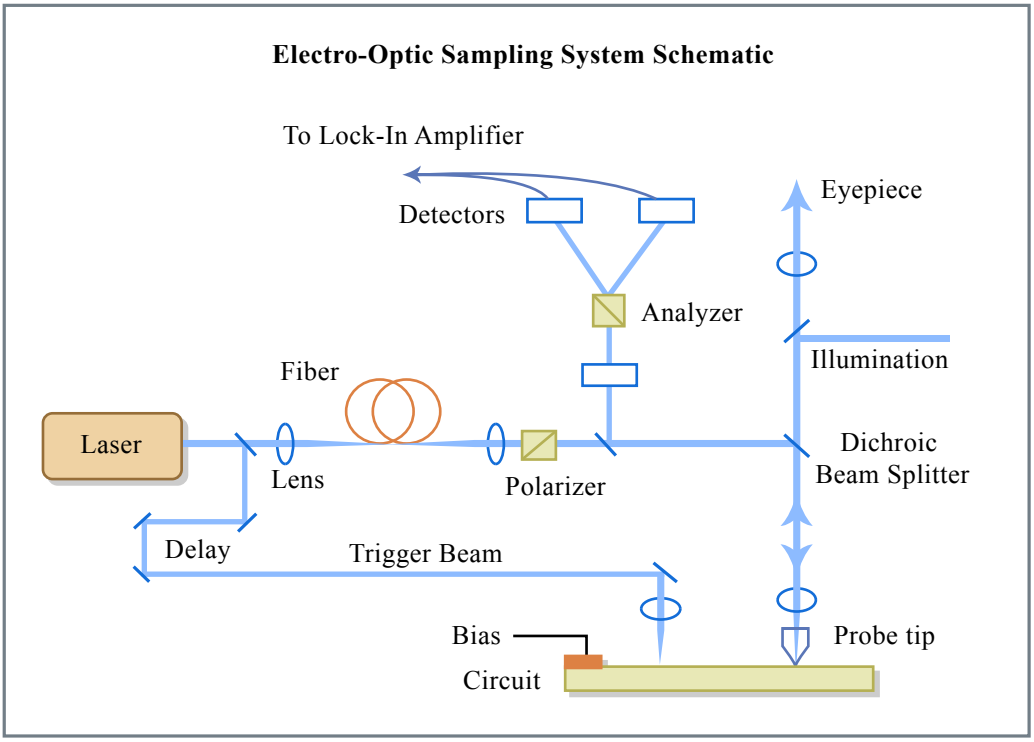

Figure 11.8: Electro-Otpic Sampling System according to J. Whitaker, Univ. Michigan.

Figure by MIT OCW.

11.3 THz Spectroscopy and Imaging

Photo-conductive switches activated by sub-100 fs pulses or optical rectification with sub-100 fs pulses leads to the generation of THz electro-magnetic impulses, that can be received with similar photo-conductive receivers or by electro-optic sampling [8][9]. This technique was pioneered by Ch. Fattinger and D. Grischkowsky [7].

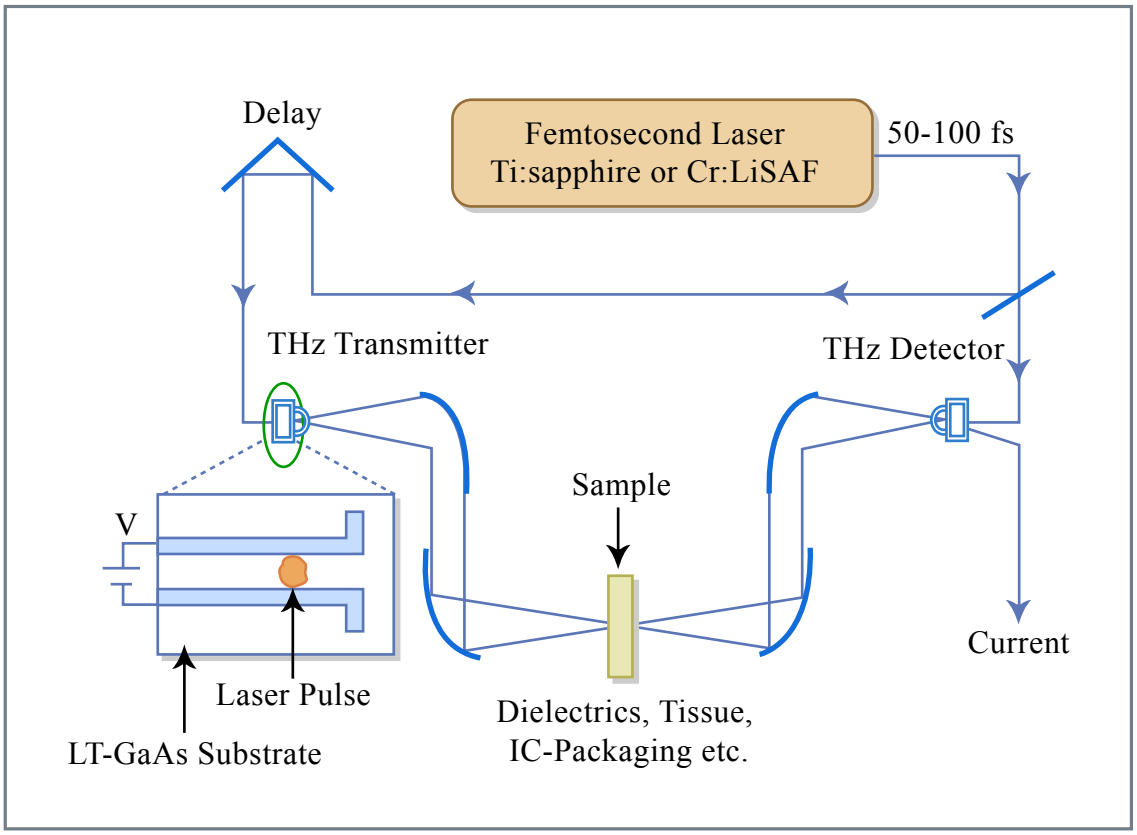

Figure 11.9: THz Time Domain Spectroscopy according to [8]

Figure by MIT OCW.

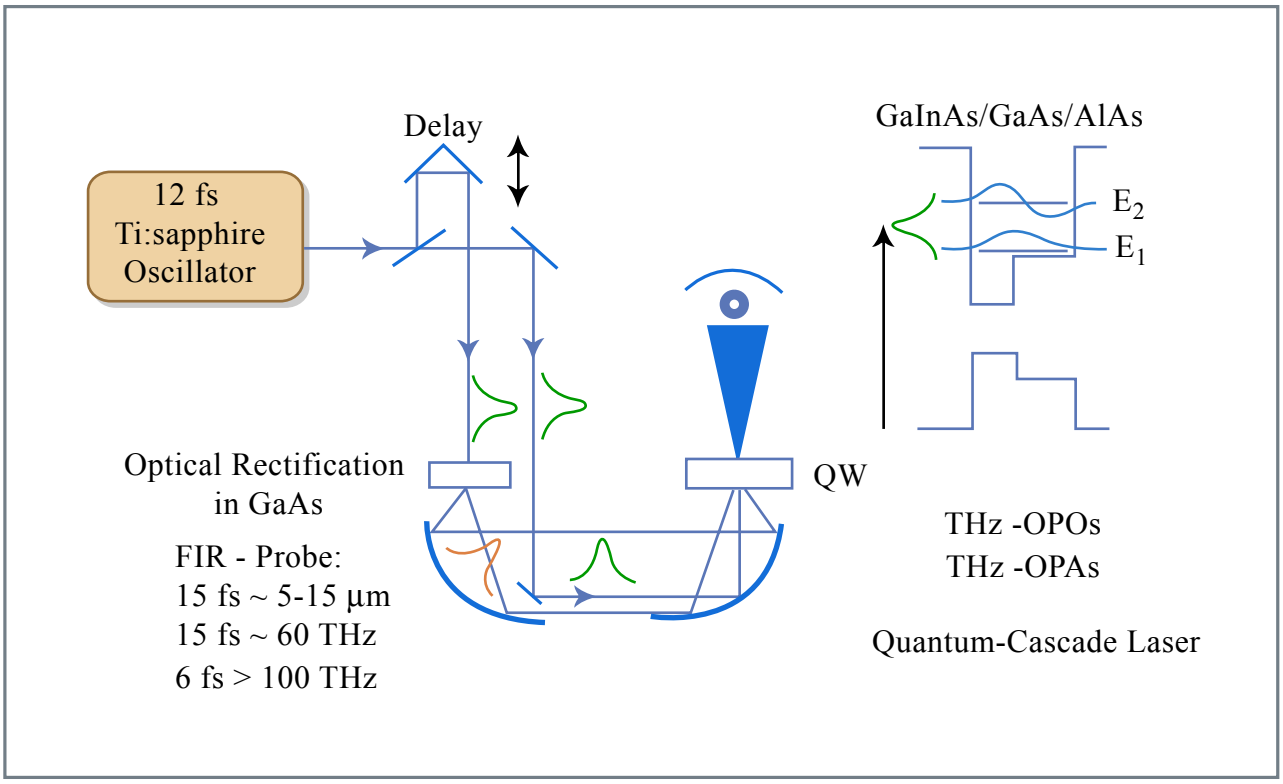

Figure 11.10: THz Time Domain Spectroscopy using optical rectification in GaAs [9].

Figure by MIT OCW.

Figure 11.11: Terahertz waveforms modified by passage through (a) a 10mm block of stycast and (b) a chinese fortune cookie. The dashed lines show the shape of the input waveform multiplied by 0.5 in (a) and by 0.1 in 9b). In *a(the transmitted plse exhibits a strong "chirp" due to frequency-dependent index, while in (b), pulse broadening indicates preferential absorption of high frequencies [8].

Figure 11.11 shows typical generated THz waveforms and distortions due to propagation through materials.

11.4 Four-Wave Mixing

A more advanced ultrafast spectroscopy technique than pump-probe is four-wave mixing (FWM). It enables to investigate not only energy relaxation processes, as is the case in pump-probe measurements, but also dephasing processes in homogenous as well as inhomogenously broadened materials. The typical set-up is shown in Fig. 11.12

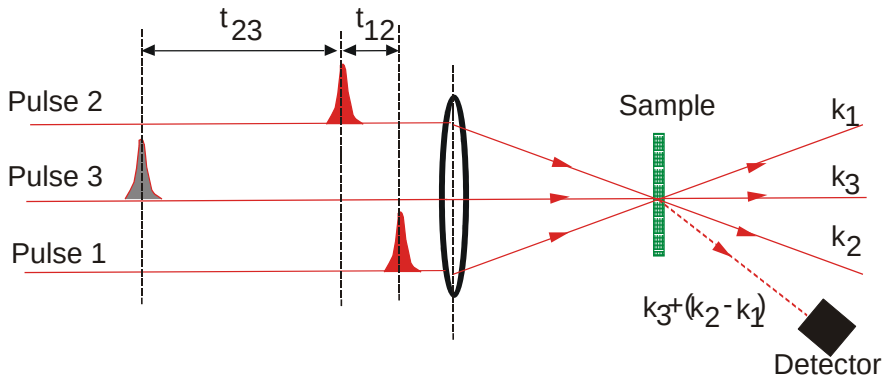

Figure 11.12: Typical Four-Wave-Mixing (FWM) beam geometry.

Lets assume these pulses interact resonantely with a two-level system modelled by the Bloch Equations derived in chapter 2 (2.1592.162).

$$\left(\Delta - \frac{1}{c_0^2}\frac{\partial^2}{\partial t^2}\right)\vec{E}^{(+)}(z,t) = \mu_0\frac{\partial^2}{\partial t^2}\vec{P}^{(+)}(z,t), \tag{11.2}$$

$$\vec{P}^{(+)}(z,t) = -2N\vec{M}^* d(z,t) \tag{11.3}$$

$$\dot{d}(z,t) = -(\frac{1}{T_2} - \mathrm{j}\omega_{eg})d + \frac{1}{2\mathrm{j}\hbar}\vec{M}\vec{E}^{(+)}w, \tag{11.4}$$

$$\dot{w}(z,t) = -\frac{w - w_0}{T_1} + \frac{1}{\mathrm{j}\hbar}(\vec{M}^*\vec{E}^{(-)}d - \vec{M}\vec{E}^{(+)}d^* \tag{11.5}$$

The two-level system, located at $z = 0$, will be in the ground state, i.e. $d(t = 0) = 0$ and $w(t = 0) = -1$, before arrival of the first pulses. That is, no polarization is yet present. Lets assume the pulse interacting with the two-level system are weak and we can apply perturbation theory. Then the arrival of the first pulse with the complex field

$$\vec{E}^{(+)}(\vec{x},t) = \vec{E}_0^{(+)}\delta(t)e^{j(\omega_{eg}t - j\vec{k}_1\vec{x})} \tag{11.6}$$

will generate a polarization wave according to the Bloch-equations

$$d(\vec{x},t) = -\frac{\vec{M}\vec{E}_0^{(+)}}{2\mathrm{j}\hbar} e^{j(\omega_{eg}-1/T_2)t} e^{-j\vec{k}_1\vec{x}} \delta(z), \tag{11.7}$$

which will decay with time. Once a polarization is created the second pulse will change the population and induce a weak population grating

$$\Delta w(\vec{x},t) = \frac{\left|\vec{M}\vec{E}_0^{(+)}\right|^2}{\hbar^2} e^{-t_{12}/T_2} e^{-j\left(\vec{k}_1-\vec{k}_2\right)\vec{x}} e^{-(t-t_2)/T_1} \delta(z) + c.c., \tag{11.8}$$

When the third pulse comes, it will scatter of from this population grating, i.e. it will induce a polarization, that radiates a wave into the direction $\vec{k}_3 + \vec{k}_2 - \vec{k}_1$ according to

$$d(\vec{x},t) = \frac{\vec{M}\vec{E}_0^{(+)}}{2\mathrm{j}\hbar} \frac{\left|\vec{M}\vec{E}_0^{(+)}\right|^2}{\hbar^2} e^{-t_{12}/T_2} e^{-t_{32}/T_1} e^{-j\left(\vec{k}_3+\vec{k}_2-\vec{k}_1\right)\vec{x}} \delta(z) \tag{11.9}$$

Thus the signal detected in this direction, see Fig. 11.12, which is proportional to the square of the radiating dipole layer

$$S(t) \sim \left|d(\vec{x},t)\right|^2 \sim e^{-2t_{12}/T_2} e^{-2t_{32}/T_1} \tag{11.10}$$

will decay on two time scales. If the time delay between pulses 1 and 2, t_{12}, is only varied it will decay with the dephasing time $T_2/2$. If the time delay between pulses 2 and 3 is varied, t_{32}, the signal strength will decay with the energy relaxation time $T_1/2$

Bibliography

[1] K. L. Hall, G. Lenz, E. P. Ippen, and G. Raybon, "Heterodyne pump-probe technique for time-domain studies of optical nonlinearities in waveguides," Opt. Lett. **17**, p.874-876, (1992).

[2] K. L. Hall, A. M. Darwish, E. P. Ippen, U. Koren and G. Raybon, "Femtosecond index nonlinearities in InGaAsP optical amplifiers," App. Phys. Lett. **62**, p.1320-1322, (1993).

[3] K. L. Hall, G. Lenz, A. M. Darwish, E. P. Ippen, "Subpicosecond gain and index nonlinearities in InGaAsP diode lasers," Opt. Comm. **111**, p.589-612 (1994).

[4] J. A. Valdmanis, G. Mourou, and C. W. Gabel, "Picosecond electro-optic sampling system," Appl. Phys. Lett. **41**, p. 211-212 (1982).

[5] B. H. Kolner and D. M. Bloom, "Electrooptic Sampling in GaAs Integrated Circuits," IEEE J. Quantum Elect.**22**, 79-93 (1986).

[6] S. Gupta, M. Y. Frankel, J. A. Valdmanis, J. F. Whitaker, G. A. Mourou, F. W. Smith and A. R. Calaw , "Subpicosecond carrier lifetime in GaAs grown by molecular beam epitaxy at low temperatures," App. Phys. Lett. **59**, pp. 3276-3278 91991)

[7] Ch. Fattinger, D. Grischkowsky, "Terahertz beams," Appl. Phys. Lett. **54**, pp.490-492 (1989)

[8] D. M. Mittleman, R. H. Jacobsen, and M. Nuss, "T-Ray Imaging," IEEE JSTQE **2**, 679-698 (1996)

[9] A. Bonvalet, J. Nagle, V. Berger, A. Migus, JL Martin, and M. Joffre, "Ultrafast Dynamic Control of Spin and Charge Density Oscillations in a GaAs Quantum Well," Phys. Rev. Lett. **76**, 4392 (1996).